Targeted *In Situ* Biosynthetic Transcriptional Activation in Native Surface-Level Human Articular Chondrocytes during Lesion Stabilization

Kumkum Ganguly[1], Ian D. McRury[2], Peter M. Goodwin[1], Roy E. Morgan[2], and Wayne K. Augé, II[2,3]

Abstract

Objective: Safe articular cartilage lesion stabilization is an important early surgical intervention advance toward mitigating articular cartilage disease burden. While short-term chondrocyte viability and chondrosupportive matrix modification have been demonstrated within tissue contiguous to targeted removal of damaged articular cartilage, longer term tissue responses require evaluation to further clarify treatment efficacy. The purpose of this study was to examine surface chondrocyte responses within contiguous tissue after lesion stabilization. *Methods:* Nonablation radiofrequency lesion stabilization of human cartilage explants obtained during knee replacement was performed for surface fibrillation. Time-dependent chondrocyte viability, nuclear morphology and cell distribution, and temporal response kinetics of matrix and chaperone gene transcription indicative of differentiated chondrocyte function were evaluated in samples at intervals to 96 hours after treatment. *Results:* Subadjacent surface articular cartilage chondrocytes demonstrated continued viability for 96 hours after treatment, a lack of increased nuclear fragmentation or condensation, persistent nucleic acid production during incubation reflecting cellular assembly behavior, and transcriptional up-regulation of matrix and chaperone genes indicative of retained biosynthetic differentiated cell function. *Conclusions:* The results of this study provide further evidence of treatment efficacy and suggest the possibility to manipulate or induce cellular function, thereby recruiting local chondrocytes to aid lesion recovery. Early surgical intervention may be viewed as a tissue rescue, allowing articular cartilage to continue displaying biological responses appropriate to its function rather than converting to a tissue ultimately governed by the degenerative material property responses of matrix failure. Early intervention may positively impact the late changes and reduce disease burden of damaged articular cartilage.

Introduction

The goal of early surgical intervention for articular cartilage damage is to stabilize lesions as a means to decrease symptoms and disease progression.[1] Lesion stabilization remains a necessary prerequisite toward articular cartilage tissue preservation because removing the irritant of damaged tissue and creating a residually healthy lesion site remain required substrates for permitting or inducing effective *in situ* healing responses. Comparative effectiveness research has demonstrated significant advances in the safety profile for articular cartilage lesion stabilization with nonablation radiofrequency technology,[a,2,3] improving evidence-based medical decision making and health care resource allocation.

[a]Although this technology platform is a derivative of alternating current redox magnetohydrodynamics[4, 5] adapted for therapeutic wound healing interventions, it has been colloquially referred to as "nonablation radiofrequency" technology due to its use of standard electrosurgical generator power and cosmetic similarities to palliative tissue resection ablation devices.

[1]Los Alamos National Laboratory, Los Alamos, NM, USA
[2]NuOrtho Surgical Inc., Fall River, MA, USA
[3]Center for Orthopaedic and Sports Performance Research Inc., Santa Fe, NM, USA

Corresponding Author:
Wayne K. Auge, Center for Orthopaedic and Sports Performance Research Inc., 936 Vista Jemez Court, Santa Fe, NM 87505
Email: infocospr@aol.com

Prior to the advent of nonablation technology for articular cartilage lesion stabilization, thermal and plasma radiofrequency ablation devices appeared to be more efficacious than mechanical shavers by exhibiting a smaller time-zero collateral injury footprint.[6-12] However, because matrix corruption and chondrocyte depletion within contiguous healthy tissue occur commensurate with, and often significantly expand following, volumetric tissue removal,[2,3,13-25] this technology did not become widely adopted, as it is understandable that such damage can impair or inhibit *in situ* healing responses[13,15,16,19,25] as well as contribute to disease progression by enlarging lesion size.[18,22,23,26-33] Despite optimizing ablation device performance, this collateral injury footprint transgresses zonal boundaries in which the depth of necrosis in nontargeted tissue remains larger than native superficial zone thickness; consequently, the functional properties and vital healing phenotype of the superficial zone are always effectively eliminated.[2,3] These collateral wounds originate because ablation technology, like mechanical shavers, cannot distinguish between damaged and undamaged tissue. Utilizing direct electrode-to-tissue interfaces indiscriminately deposits current into tissue, which causes surface entry wounds and subsurface necrosis through resistive tissue heating and tissue electrolysis; also, because of its high water content, articular cartilage is inherently at risk for efficiently pooling electrothermal energy to a detrimental level. Some have advocated manually positioning the active electrode away from healthy tissue to target diseased tissue[34,35]; however, this technique significantly increases the amount of current required to overcome the effects that the fluid flow and convective forces present during surgical application exert on exposed device electrodes. Others have offered that intentional current-based damage serves as a barrier to additional current deposition without demonstrating damage efficacy.[20] Still others utilize current to create ionizing electromagnetic radiation associated with high temperature plasma formation,[36-39] which has raised further concerns regarding iatrogenic chondrocyte DNA fragmentation and nuclear condensation that can induce apoptosis,[40] cellular senescence,[41] decreased[42] progenitor cell populations,[43-47] diminished cellular differentiation potential,[42] and altered extracellular matrix structure and production.[48] Additional effects of ionizing electromagnetic radiation on chondrocyte behavior important for *in situ* healing responses[49-57] remain worrisome.

Nonablation technology enables selective targeting of diseased tissue traits by utilizing a protected electrode architecture that prohibits electrode-to-tissue contact as a means to eliminate volumetric and functional overresection that further impairs contiguous healthy tissue from retaining and displaying differentiated phenotypes.[2,3,58-60] The protective housing creates a primary reaction zone that is shielded from the large physical fluid flow and convective forces present during surgical application, enabling deployment of low-level radiofrequency energy delivery into interfacing media rather than into tissue to create physiochemical conversions that can be used for surgical work. This process creates an engineered irrigant that physiochemically loads tissue surfaces in a manner uniquely suited to effect the accessible and degenerate surface matrix structure of damaged articular cartilage tissue preferentially rather than the intact chondron and matrix tissue deep to the surface lesion level. As an illustration, pH shifts can be generated, such as preferential sodium hypochlorite precipitation akin to production through neutrophil myeloperoxidase catalysis, and configured to react oxidatively with a wide variety of biomolecules at tissue surfaces including the exposed proteoglycan aggregates of damaged articular cartilage.[61-63] Such proton charge shifts have been shown to produce mechanical alterations at articular cartilage surfaces[2,3] through electrochemomechanical coupling via site-specific hydrogen and disulfide bond alterations within constituent proteoglycan and collagen.[64-69] These targeted gradients at tissue surfaces modulate mechanical and electrochemical tissue matrix properties by altering fixed and variable charge densities while effecting consequent extracellular intrafibrillar hydration and osmotic character.[70-79] This physiochemical loading of accessible surface-based diseased tissue can alter the relative ratio of tension compression nonlinearity toward a state amenable to gentle shear deformation mechanical debridement of tissue already characterized by the deteriorating surface-layered shear properties of collagen fibril disruption and orientation changes, weak collagen-to-proteoglycan bonds, proteoglycan and lipid depletion, aberrant water content, and decreased fixed charge density.[80-84] Optimizing the surface shear properties of early articular cartilage damage through cleavage plane stabilization is an important parameter for overall lesion stabilization relative to perturbation specificity[58] particularly because these mechanisms do not impair residual chondrocyte viability.[2,3,85] These layered surface properties exploited for cleavage plane shear stabilization have been observed in other tissue types and locales requiring shear mitigation during surface degeneration and normally represent a back-up mechanism to boundary lubrication regime failures associated with perturbation exceeding homeostasis and tissue repair for reversible lesions.[56,86]

It has been demonstrated previously that nonablation technology selectively targets diseased tissue for removal without causing necrosis in contiguous healthy cartilage tissue while producing the chondrosupportive matrix modification of increased live chondron density in the superficial zone.[2,3] Because chondrocyte viability in subadjacent tissue is not altered, the opportunity presents to evaluate chondrocyte behavior in response to lesion stabilization. The purpose of this study was to examine the focal effects upon residual articular cartilage surface chondrocytes during lesion stabilization with nonablation technology by

evaluating time-dependent chondrocyte viability, nuclear morphology and cell distribution, and temporal response kinetics of matrix and chaperone gene transcription indicative of differentiated chondrocyte function.

Materials and Methods

Study Design, Human Tissue Specimens, and Nonablation Treatment

Because eliminating articular cartilage overresection has been enabled for patients only recently, this study was designed as an exploratory assessment of an experimental explant model that represents human disease while not requiring *in vivo* biopsies of preserved tissues (contrary to the goal of eliminating overresection) to simultaneously evaluate intrapatient measures of both volumetric and functional overresection. Mutually confirmatory testing methods across 3 investigational categories were included with paired controls in order to gather a broad and interrelated data range representing residual contiguous chondrocyte viability and differentiated function. As an exploratory assessment, and prior to extending to other human subjects an experimental tissue injury model that includes access to a patient's personal genetic information,[87] this study sought to evaluate the model in a single patient displaying the opportunity for uniform articular cartilage lesion sampling of a sufficient combined geographic area necessary to complete the multiple testing procedures with appropriate model test-method repeatability replicates. As an initial benchmark, articular cartilage samples were evaluated at 1 hour (earliest postharvest treatment-processing time) through 96 hours (after which chondrocyte responses can be more reflective of incubation environment rather than the treatment method[88]).

Osteochondral specimens were harvested from patients undergoing total knee replacement under an approved Human Subjects Research and Institutional Review Board protocol that included informed written patient consent. The total knee replacement procedures were performed by a single surgeon in the normal course of his practice. The tissue to be normally discarded during the procedure was examined prior to harvest once the knee joint was entered surgically to determine if it met study inclusion requirements. Specimens were included that demonstrated an area of uniform partial-thickness surface fibrillation of sufficient size from which matched-pair test samples could be obtained from each specimen. Specimens were divided into smaller test sample parts after harvest by sharp sectioning and were immediately transferred to an *ex vivo* saline arthroscopic treatment setting. The individual specimens of each matched pair were randomized as to which remained untreated or became treated.

A nonablation radiofrequency device designed for cartilage lesion stabilization was used per the manufacturer's specifications (Ceruleau, NuOrtho Surgical Inc., Fall River, MA). Lesion stabilization was performed by one surgeon accustomed to device use. The goal of the procedure was to remove the fibrillated cartilage damage and smooth the articular surface as determined by visual and tactile cues. Standard saline arthroscopic fluid was deployed at 20 °C with a fluid flow rate of 30 mL/min ± 5 mL/min, which created consistent fluid dynamics in the setup typical of *in vivo* arthroscopy. Energy delivery (Valleylab Force FX-C, Covidien Inc., Mansfield, MA) was standardized at 25 W with an 8,500-V peak-to-peak setting (4,250 peak voltage) and 390-kHz damped sinusoid bursts with a repetition frequency of 30 kHz into 500 ohms (i.e., COAG, fulgurate). Lesion stabilization treatment time was 5 seconds for all specimens, with a technique of moving the probe tip tangentially across the tissue surface with a consistent application pressure and speed as judged by the surgeon to mimic *in vivo* treatment conditions. The protective housing edge was used to gently shear-debride the fibrillated tissue concurrent with energy delivery for the allotted treatment time. This technique did not deploy the heat delivery capabilities of nonablation technology available through electrosurgical plenum positioning or increased energy levels that can be used[58] for the more demanding lesion stabilization associated with less fibrillated tissue displaying a different degeneration-based collagen fibril-to-water structure (see Discussion); as deployed in this study, the delivery of heat to tissue surfaces is limited by a triphasic nature to low temperature changes (i.e., Δ 0-7 °C) of interfacing media,[58] which is design appropriate for the low thermal requirements that would be necessary to manipulate exposed surface type II collagen, which begins to denature at 39 °C. Paired sample explants served to generate untreated samples to serve as control that remained in an identical treatment bath during the procedure. After treatment, the matched-pair samples were randomly divided into 3 groups for evaluation of time-dependent chondrocyte viability, nuclear morphology and cell distribution, and temporal kinetics of versican, COL2A1, and HSPA1A gene expression in surface chondrocytes.

Evaluation of Time-Dependent Chondrocyte Viability

The samples allocated to this group were evaluated at 1-hour and 96-hour intervals after treatment for alterations in chondrocyte viability. Samples were prepared by thin sectioning to isolate the surface region containing superficial and transitional zone chondrocytes and matrix from the remainder of the tissue (sample dimensions: 3-mm thick by 7-mm square). These surface cartilage specimens were left

as bulk tissue and incubated at 37 °C in Dulbecco's Modified Eagle's Medium (Invitrogen Inc., Carlsbad, CA) with fetal bovine serum and 1% penicillin-streptomycin (10,000 U and 10,000 µg, respectively). No equilibration period was used, and the specimens were incubated in 95% air with 5% CO_2. At 1 hour and 96 hours, three 0.5-mm coronal sections of each sample referencing the center of the untreated and treated sites were created and prepared for staining by washing in HEPES buffered saline solution. Live/Dead Reduced Biohazard Cell Viability Kit #L-7013 (Invitrogen Inc.) was used per the manufacturer's specification to stain samples. Samples were gluteraldehyde fixed, transferred to standard flat glass slides, and flooded with VectaShield fluorescence protection oil (Vector Laboratories, Inc., Burlingame, CA) prior to the placement of No. 1.5 borosilicate glass cover slips over each sample section.

Confocal fluorescence laser microscopy analysis was performed by personnel blinded to the identity of the treatment groups for each sample. Confocal imaging was performed with an IX-81 inverted microscope coupled to a FV300 confocal laser-scanning unit (Olympus Inc., Center Valley, PA) using continuous-wave 488-nm laser excitation (Sapphire 488HP, Coherent Inc., Santa Clara, CA). Live cells were captured under the green fluorescence channel (505-525 nm), and dead cells were captured under the red fluorescence channel (577-634 nm), generating a live image, a dead image, and an integrated image. Histological characteristics and cell viability between untreated and treated samples were assessed by comparative image evaluation for change in live and dead cell populations.

Nuclear Morphology and Cell Distribution

The samples allocated to this group were evaluated at the 1-hour posttreatment interval to determine alterations in nuclear morphology and cell distribution. Samples were maintained after treatment in the arthroscopic saline bath and prepared by thin sectioning and incubated as above. Because significantly altered nuclear characteristics would not be expected in the presence of continued differentiated nucleic acid production over time, incubated samples would only be evaluated at 96 hours should continued gene expression not be observed in both untreated and treated samples (as described below) in order to assess possible transcriptional failure modes. Three 0.5-mm coronal sections of each sample referencing the center of the treatment site and control were created and prepared for staining by washing in HEPES buffered saline solution. Hoechst 33342 stain, trihydrochloride FluoroPure (#H-21492, Invitrogen Inc.), was used per the manufacturer's specification to stain samples. Samples were fixed and prepared for imaging as above.

Two-photon excitation microscopy was performed with an IX-81 inverted microscope coupled to a FV300 confocal

laser-scanning unit (Olympus Inc.) using a 60x 1.2-NA water immersion objective (UPLSAPO 60XW, Olympus Inc.) for imaging. A dichroic mirror that reflected the near-infrared laser excitation light and transmitted the visible (~460 nm) bisbenzimide emission was used as the excitation dichroic. The excitation source was a mode-locked titanium sapphire laser (Broadband Mai Tai, Spectra Physics, Newport Inc., Irvine, CA) operating at 800 nm with a pulse width of approximately 100 fs and a pulse repetition rate of 80 MHz. An average power of approximately 30 mW (measured at the back aperture of the microscope objective) was used to excite the sample emission. A short-pass filter with a cut-off wavelength of 680 nm (FF01-680/SP, Semrock Inc., Rochester, NY) was used to filter residual 800-nm excitation laser light from the emission. Water was used as an immersion fluid to optically couple the sample and objective to the cover slip.

Serial x-y plane tomographic images along the z-axis were generated to evaluate nuclear morphology and cell distribution. Dye exclusion properties were not evaluated. These images were compressed into a single x-y image combining the nuclear contents along the z-axis image planes into a single composite view to facilitate additional interchondrocyte nuclear comparisons. BioView open-source cross-platform application software (Center for Bio-Image Informatics, University of California, Santa Barbara, CA) was used to evaluate cell distribution patterns because all sample chondrocyte nuclei stain with bisbenzimide. Axis rotations were performed to evaluate matrix modifications of treated versus untreated samples that may affect cell distribution patterns as noted previously.[3]

Evaluation of Matrix and Chaperone Gene Expression by Real-Time Polymerase Chain Reaction (RT-PCR)

The samples allocated to this group were prepared by thin sectioning (sample dimensions: 2-mm thick by 5-mm square) and incubated as above. Untreated and treated samples were randomly assigned to incubation intervals of 1, 24, 48, 72, and 96 hours. At the end of each incubation interval, the samples were frozen in liquid nitrogen and stored at –80 °C prior to RT-PCR testing. At testing, the samples were thawed and mechanically homogenized in lysis reagent (QIAzol #79306, Qiagen Inc., Valencia, CA). The homogenate was separated into aqueous and organic phases by centrifugation, and mRNA was subsequently isolated by spin column elution (RNeasy Lipid Tissue Mini Kit #74804, Qiagen Inc.).

Quantitative reverse transcriptase RT-PCR was performed (7300 Real-Time PCR System, Applied Biosystems Inc., Carlsbad, CA) by monitoring the increase in reporter fluorescence of Taqman gene expression assays (Applied

Biosystems Inc.) for versican (#Hs00171642_m1), COL2A1 (#Hs00264051_m1), and HSPA1A (#Hs00359163_s1). RNA concentration obtained was determined for both untreated and treated samples and evaluated for significant differences; sample purity was evaluated for each specimen by determining $R_{260/280}$ values (ultraviolet absorbance ratio at 260 nm and 280 nm). Expression changes were quantified by the comparative C_T method to calculate relative fold changes normalized against 18s rRNA, calculated as the difference (ΔC_T) between the C_T value of the target and 18s rRNA control. Each sample was assayed in duplicate with relative expression calculated and tabulated as $2^{-\Delta\Delta CT}$ relative to each incubation interval sample group. The mean and standard deviation were calculated for each fold change grouping. Curve fit regression analysis for mRNA expression temporal kinetic fold change was performed (TableCurve 2D, version 5.01.02, Systat Software Inc., Chicago, IL) for the treated sample groups compared to the average ΔC_T of the 1-hour untreated sample group serving as control and as time zero designed to demonstrate the relative scale of expression responses over time.

Results

Study Design, Human Tissue Specimens, and Nonablation Treatment

The tissue samples for this study were donated by a 59-year-old female patient diagnosed with symptomatic bilateral knee primary osteoarthritis and without prior surgical cartilage treatment. Articular cartilage tissue sampling was generated from femoral condyle, tibial plateau, and patella locations that demonstrated consistent intersite surface fibrillation as judged by arthroscopic-magnified visual and tactile cues and that retained a gross harvest site cartilage thickness of at least 3 mm, conditions indicative of the diseased state studied. Matched-pair samples were successfully created and randomized into the 3 investigational categories. The general results across these categories demonstrated corroborating model validation of the mutually confirmatory testing methods included in this experimental explant model, signifying residual contiguous chondrocyte viability and differentiated behavior without evidence of volumetric or functional overresection.

Evaluation of Time-Dependent Chondrocyte Viability

Four matched-pair samples were allocated to this group, 2 for each time interval. The untreated samples demonstrated surface fibrillation consistent with gross visual inspection of the tissue at the time of harvest. The superficial zone was disrupted by the fibrillation, but chondron appearance typical of this zone remained present in and around the fibrilla-
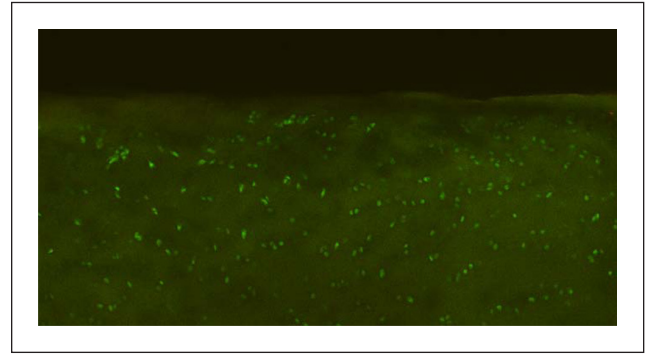

Figure 1. Representative posttreatment integrated live/dead cell viability stain section image, demonstrating viable chondrocytes. Note the lack of dead chondrocytes and a smooth surface in the tissue subadjacent to the targeted removal of surface-fibrillated tissue damage. Original magnification, 10x.

tion. Live cells were abundantly observed with only occasional dead cells residing in extruded positions at the frayed margins of the fibrillated tissue. Treated samples displayed elimination of the fibrillated tissue and smooth surfaces at the treatment site. No evidence of necrotic tissue was present with the surfaces subadjacent to the removed damaged tissue retaining superficial zone characteristics typical of the intact superficial zone regions of the untreated samples. An increase in dead cell populations was not evident in either the 1-hour or the 96-hour treated samples over the untreated sample groups, nor was a decrease in chondrocyte viability observed relative to incubation time. **Figure 1** depicts a representative posttreatment integrated live/dead cell viability stain section image, demonstrating surface characteristics and viable chondrocytes without evidence of necrosis or altered cellular viability.

Nuclear Morphology and Cell Distribution

Four matched-pair samples were allocated to this group, 2 for each time interval. Due to the presence of continued gene expression in both untreated and treated samples (as described below), evaluation was not performed at the 96-hour time interval. The serial tomographic images demonstrated no evidence of altered nuclear morphology when compared to untreated samples. As depicted in **Figure 2**, nuclear fragmentation or condensation (i.e., peripheral segregation or aggregation of chromatin into dense areas along the nuclear membrane) was not present within the tissue chondrocytes subadjacent to the tissue targeted for removal, reflecting no evidence of chondrocyte apoptosis. Cells typically contained a large nucleus with loosely packed euchromatin and little more dense heterochromatin. Homogeneous staining intensities appeared uniform in the z-axis compressed images. Occasional single randomly

Figure 2. Representative 2-photon confocal composite image of Hoechst-stained chondrocytes with the tomographic z-axis images compressed into a single image. Note the similar staining intensities and lack of nuclear fragmentation or condensation. Original magnification, 60x water.

positioned cells demonstrated altered nuclear morphologies in some untreated and treated samples, which could not be linked to the treatment site and likely represented fixation-dependent or other causes typical within articular cartilage. **Figure 3** depicts representative BioView images (Center for Bio-Image Informatics, University of California, Santa Barbara) of cell distribution viewed from the x-y, x-z, and y-z vantage points. Axis rotation assessments indicated evidence of qualitative extracellular matrix contraction in the tissue immediately contiguous to the tissue targeted for removal and within the superficial zone region when compared to untreated samples. **Supplementary Figure S1** is a representative video depicting x-y-z coordinate results of lesion stabilization used to assess extracellular matrix modifications.

Evaluation of Matrix and Chaperone Gene Expression by Real-Time Polymerase Chain Reaction (RT-PCR)

Twenty samples were allocated to this group, generating 2 untreated and treated paired sample explants for each incubation interval. The RNA quantity obtained included an untreated group concentration of 29.8 ± 9.3 ng/μL and a treated group concentration of 29.7 ± 8.6 ng/μL, with no statistical differences between groups. As depicted in **Figure 4**, $R_{260/280}$ values were 1.76 ± 0.06 and 1.76 ± 0.10 for untreated and treated samples, respectively, with no
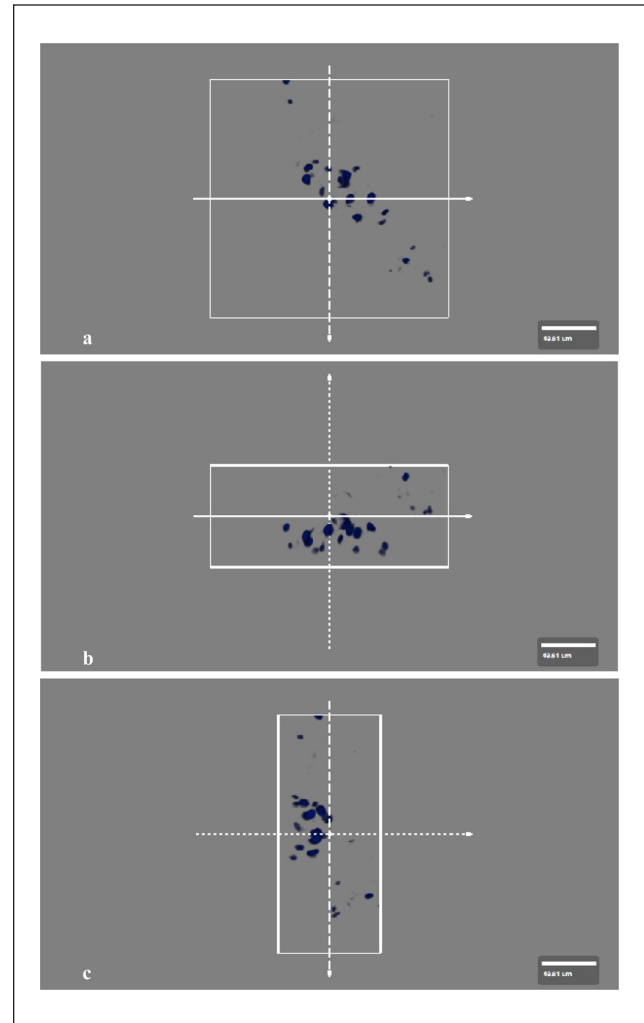

Figure 3. Representative BioView images used to assess 3-dimensional chondrocyte distribution patterns. (**A**) The x-y plot, (**B**) the x-z plot, and (**C**) the y-z plot. Solid, dotted, and dashed lines with arrows reflect coordinate orientation between the images displayed.

statistical significance between groups at each time period during the incubation.

Figure 5 depicts the fold change temporal kinetics of versican, COL2A1, and HSPA1A mRNA expression. The untreated sample group continued to express a stable mRNA level during incubation and did not demonstrate significant fold change variations during the incubation period in any of the mRNAs examined. The treated sample group demonstrated a large fold increase in expression early followed by a reversion to baseline expression comparable to untreated samples. Versican mRNA was undetectable at 96 hours in the treated samples, and its standard deviation at the 24-hour incubation interval was large. **Figure 6** depicts curve regression fit of the expression events based on concentration kinetic changes modeled as single production versus single
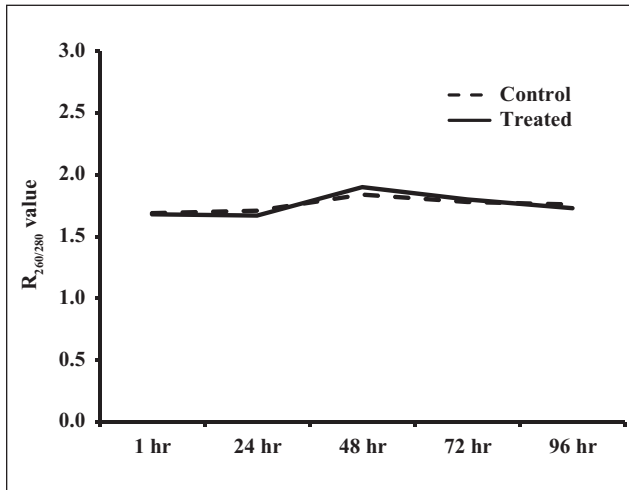
Figure 4. R$_{260/280}$ values versus time. Note the stability of RNA sample purity produced during the testing period for each incubation interval.
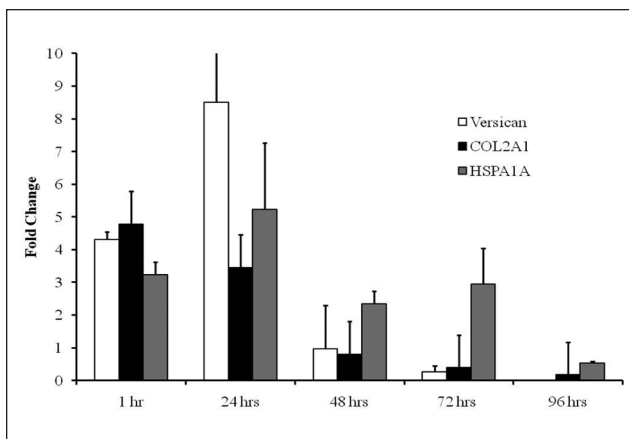

Figure 5. RT-PCR results depicting mean fold changes in transcriptional expression of versican, COL2A1, and HSPA1A mRNA in subadjacent surface chondrocyte after nonablation radiofrequency lesion stabilization. Data reflect fold change relative to the untreated samples at each incubation interval.

removal rates. The curve regression fit was statistically significant, with strong relevance for versican ($R^2 = 0.72$; $P < 0.04$), COL2A1 ($R^2 = 0.92$; $P < 0.0004$), and HSPA1A ($R^2 = 0.83$; $P < 0.002$), demonstrating a scaled temporal response similar to the fold change assessment based upon the control of each incubation interval.

Discussion

Because early posttreatment chondrocyte viability is not effected within tissue contiguous to the treatment site during nonablation radiofrequency lesion stabilization,[2,3] this study was designed to further delineate treatment effi-
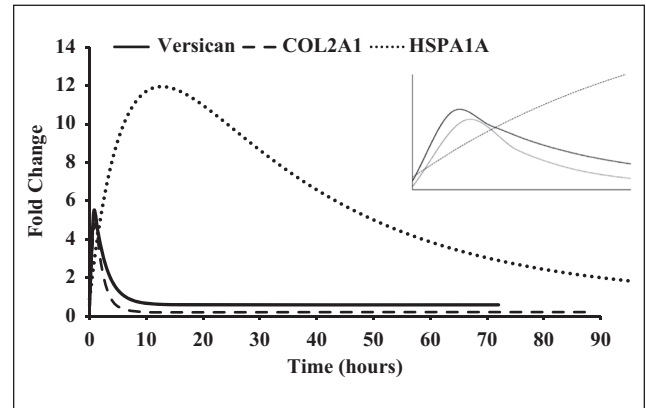

Figure 6. Curve fit regression depicting transcriptional up-regulation in subadjacent surface chondrocytes after nonablation radiofrequency lesion stabilization. Note that the high statistical fit reflects a biological phonomenon of damped exponential activation and deactivation/reaction exhaustion. Inset depicts an enlarged view of the modeled temporal expression kinetics after treatment. Data reflect treated sample groups compared to the average ΔC_T of the 1-hour untreated sample group serving as control and as time zero.

cacy through an exploratory assessment of chondrocyte experiences during and in reaction to lesion stabilization. Subadjacent surface articular cartilage chondrocytes demonstrated continued viability for 96 hours after treatment, a lack of increased nuclear fragmentation or condensation, persistent nucleic acid production during incubation reflecting cellular assembly behavior, and a transcriptional up-regulation of matrix and chaperone genes indicative of retained biosynthetic differentiated cell function. These results add to the emerging efficacy of early surgical intervention, namely, to safely eliminate the irritant of damaged tissue without iatrogenic injury to contiguous tissue,[2,3] to stabilize the remaining healthy tissue through chondrosupportive matrix modifications,[3] and to induce an appropriate *in situ* biosynthetic cellular response within the tissue subadjacent to the lesion that retains differentiated function. While removing the irritant of damaged tissue may slow lesion progression[26-33] and permit local homeostatic and repair responses[57] to occur less encumbered, the results of this study suggest that it is possible to manipulate or induce cellular function, thereby recruiting local chondrocytes to aid lesion recovery. As additional information is generated, early surgical intervention may become viewed as a tissue rescue, allowing articular cartilage to continue displaying biological responses appropriate to its function rather than converting to a tissue ultimately governed by the degenerative material property responses of matrix failure. If so, early intervention would impact the late changes and disease burden of damaged articular cartilage.

Versican mRNA expression was evaluated in this study because it is translated into a chondroitin sulfate proteoglycan

that resides as aggregates within the interterritorial matrix at articular surfaces.[89,90] This site specificity reflects its functional role in the superficial zone extracellular matrix structure[89,91] and therefore influences matrix failure–based lesion stabilization of early cartilage damage. Versican displays low chondroitin sulfate density and sulfation levels,[89,91] a property reflected in the fixed charge density inherent in surface cartilage amenable to modification by physiochemical loading during nonablation treatment. Because surface-damaged articular cartilage displays an altered fixed charge density due to layered proteoglycan depletion,[83,92] this exposed and accessible charge density is an important therapeutic target during the surface events of lesion stabilization because the normal charge barrier[93] associated with the amorphous layer is functionally abolished in damaged articular cartilage surfaces.[94] Boundary lubrication regimes[95,96] at normal articular cartilage surfaces provide a unique charge density barrier due to surface-active phospholipids, which is remarkably resistant to the physiochemical loading deployed during lesion stabilization particularly at sites bathed in sodium chloride[97-100] as during arthroscopy. This charge density serves as a physiochemical loading barrier to and an intrinsic margin during the surface events of lesion stabilization at intact surfaces, a barrier that is robust enough[95] to require enzymatic digestion, trauma, or other means like ablation energy to transgress in order to reach a collagen layer. The transient versican mRNA transcriptional up-regulation noted in response to lesion stabilization is consistent with prior studies demonstrating posttreatment superficial zone phenotype characteristics[2,3] and may be important in the reconstitution of cartilage surface properties by chondrocytes[43-47,51-57] after removal of the damaged tissue irritant. More intriguing, however, is that various isoforms of versican have been implicated in actions related to chondrogenesis through mesenchymal condensation, cell aggregation, chondroprogenitor cell promotion, and chondrocyte gene expression.[91,101-104] Because the adult isoform core protein size does not seem to change with osteoarthritis,[90] and combined with the evidence for superficial zone progenitor cell populations[43-47,91] and chondrocyte proliferation and clustering in early and fibrillated cartilage damage,[91,92] versican's posttranslational role during early tissue responses to lesion stabilization may relate to a protective, and possibly transitional, matrix construct during tissue assembly repair events by modulating chondrocyte adhesion, morphology, proliferation, differentiation, or migration[105,106] similar to its function noted during repair and self-assembly events in other tissue types.

The COL2A1 gene encodes the α-1 chain of type II collagen, the major collagen constituent of articular cartilage matrix and a good marker of an activated functional phenotype. The transcriptional enhancement of COL2A1 after targeted lesion stabilization demonstrated in this study serves as an assessment of the generalized chondrocyte function to promote articular cartilage–specific matrix synthesis. Chondrocytes at the site of lesion stabilization retain the ability to produce mRNA reflective of their differentiated phenotype and characteristic of mature cartilage, indicating that the responses are not limited to a fibroblastic-like dedifferentiation and low matrix gene expression reflective of the phenotypic alterations of diseased tissue[92] or other cartilage interventions[107] during which chondrocytes continue to express synthetic activity after treatment.[108] Further evaluation of this response, such as splice variants indicative of a chondroprogenitor phenotype,[109] would be interesting in light of the corresponding versican response temporal kinetics noted in this study.

HSPA1A codes for highly conserved nonsteric molecular chaperones that participate in protein stabilization and assembly by mediating folding and transport of existing or newly translated proteins. Chaperone levels are modulated to reflect the status of protein folding requirements within the cell such as preventing newly synthesized proteins and assembled subunits from aggregation into nonfunctional structures that can occur due to natural macromolecular crowding. Chaperone levels reflect cellular requirements related to biosynthetic responses as a means to monitor changes in cell environment.[110-112] In chondrocytes, HSPA1A proteins induce chondroprotection against apoptosis[113,114] and help resist the extracellular matrix destruction of osteoarthritis.[115,116] HSPA1A is constituently expressed in chondrocytes,[117] while its inducible expression has been related to the terminal differentiation of chondrocytes[118] and is increased in osteoarthritis as an early marker.[119,120] Although it is presently uncertain if the translational products of versican and COL2A1 are routine protein clients of HSPA1A chaperones within human articular chondrocytes, HSPA1A expression in this study is consistent with the temporal expression kinetics similar to other studies that have linked HSPA1A up-regulation with active matrix production and the reconstruction of chondrons.[121]

It is possible that removal of damaged tissue itself can enable biosynthetic activity *in vivo* as an unburdened homeostatic or repair response. By removing a biological and mechanical irritant, the lesion site can be altered to a more favorable perturbation-specific mechanotransductive environment supportive of differentiated gene expression.[122-128] However, because the tissue in this study was incubated in an unloaded state not reflective of physiological perturbation specificity,[129] it remains unclear whether the removal of the damaged tissue itself is a signaling mechanism responsible for the increased biosynthetic activity observed. Although the untreated group reflected responses of surface-fibrillated articular cartilage incubated in an unloaded environment without significant alteration in baseline mRNA expression studied, the treated samples reflected differentiated biosynthetic function consistent with normal physiological responses. The signaling

mechanisms for these responses are unlikely directly related to the physiochemical loading of the cartilage surfaces utilized during lesion stabilization. For instance, because the physiochemical loading deployed in this study did not include heat delivery,[58,59] HSPA1A induction should not be related to temperature stress, as up-regulation in chondrocytes does not occur until temperatures exceed 39 °C,[130] a temperature that interestingly is consistent with when exposed but normal extracellular matrix type II collagen begins to denature[131] and that can be deployed in a controlled manner by nonablation technology[58] for more demanding lesions.[132] Further, and although extracellular pH changes can effect chondrocyte metabolism in culture,[133] chondrocytes are not subjected to extracellular alterations in pH during short-term topical loading in sodium chloride environments.[97-100] Because nonionizing electromagnetic forces are generated by nonablation devices to promote therapeutic biological responses in tissues unencumbered by necrosis-inducing current deposition,[2,3,56,134] these forces should be considered a plausible induction mechanism at least partly responsible for the biosynthetic temporal response kinetics observed in the treated samples.[60,134-140] Such fields influence dipole moments, charge movements, and ion transporters that regulate cell function, proliferation, differentiation, and migration[135,141-143] and, when applied to cartilage, have been shown to be chondroprotective, to reduce lesion progression, and to increase chondrocyte proliferation, lacuna formation, gene expression, protein synthesis, and extracellular matrix production.[144-152] Electromagnetic forces demonstrate activity at independent gene initiation promoter domains through signaling pathways that enable short exposures to induce rapid DNA activation, a mechanism linking protein synthesis to electron charge transport acceleration induced by electromagnetic forces.[153,154]

Early intervention for articular cartilage damage remains an attractive approach to decrease disease burden because it is this setting that retains the elements *in situ* for normal cartilage homeostasis and repair. Studies examining chondrocyte behavior in culture provide important insight into concepts for *in situ* cartilage treatment[108,121,155]; maintaining chondrocytes in their normal *in vivo* position preserves their interactions with their extracellular matrix,[156,157] an important factor to consider for specific disease-state interventions. While the hallmarks of nonreversible articular cartilage lesions are more obvious, the characteristics of self-repair and regeneration at reversible lesion sites and those relative to salvageable lesions are not yet as recognizable as specific disease states.[158-160] Despite the heterogeneity of articular cartilage lesions, chondrocyte viability and a differentiated and healing phenotype at the site of safe damaged tissue removal remain inextricably related to the reversibility of early lesions. Removal of this irritant relative to

perturbation specificity is necessary to provide a more favorable environment to express mechanotransductive genes for biosynthesis while interrupting phenotypic shifts persuaded by loading an unhealthy site and, furthermore, for targeted *in situ* manipulation of those genes. Even more exciting is the potential to allow boundary lubrication regimes that are depleted with damage[161,162] to reconstitute over a nonirritated site via self-assembly[163] that may ultimately become a regional substrate for cell-homing techniques reflective of tissue assembly, homeostasis, and repair[54,57,164] enabled by eliminating volumetric and functional overresection.

Declaration of Conflicting Interests

The authors IDM, REM, and WKA have declared potential conflicts of interest with respect to the authorship and/or publication of this article.

References

1. Ganguly K, McRury ID, Goodwin PM, Morgan RE, Augé WK. Native chondrocyte viability during cartilage lesion progression: normal to surface fibrillation. Cartilage. 2010; 1:306-11.

2. Ganguly K, McRury ID, Goodwin PM, Morgan RE, Augé WK. Histopomorphic evaluation of radiofrequency mediated débridement chondroplasty. Open Orthop J. 2010; 4:211-20.

3. Ganguly K, McRury ID, Goodwin PM, Morgan RE, Augé WK. Manipulative structural re-organization of superficial zone extracellular matrix: articular chondron density increases in response to non-ablation radiofrequency energy. Cartilage. 2010;1:108S.

4. Augé WK. Inverse mass ratio batteries: an in situ energy source generated from motive proton delivery gradients. Nano Energy 2011; doi:10.1016/j.nanoen.2011.12.005.

5. Augé WK, McRury ID. Redox magnetohydrodynamic engineered irrigants (transportable regionally structure-altered water) are based upon constituent charge-to-mass ratio profiles: radiofrequency electromagnetic energy

produces a Lorentz force generated proton delivery gradient in saline associated with biologic-appropriate motive forces. Proceedings of the Sixth Annual Conference on the Physics, Chemistry, and Biology of Water. West Dover, Vermont; October 20-23, 2011.

6. Edwards RB, Lu Y, Cole BJ, Muir P, Markel MD. Comparison of radiofrequency treatment and mechanical débridement of fibrillated cartilage in an equine model. Vet Comp Orthop Traumatol. 2008;21:41-8.

7. Edwards RB, Lu Y, Uthamanthil RK, Bogdanske JJ, Muir P, Athanasiou KA, et al. Comparison of mechanical débridement and radiofrequency energy for chondroplasty in an in vivo equine model of partial thickness cartilage injury. Osteoarthritis Cartilage. 2007;15:169-78.

8. Kang RW, Gomoll AH, Nho SJ, Pylawka TK, Cole BJ. Outcomes of mechanical débridement and radiofrequency ablation in the treatment of chondral defects: a prospective randomized study. J Knee Surg. 2008;21:116-21.

9. Lotto ML, Wright EJ, Appleby D, Zelicof SB, Lemos MJ, Lubowitz JH. Ex vivo comparison of mechanical versus thermal chondroplasty: assessment of tissue effect at the surgical endpoint. Arthroscopy. 2008;24:410-5.

10. Owens BD, Stickles BJ, Balikian P, Busconi BD. Prospective analysis of radiofrequency versus mechanical débridement of isolated patellar chondral lesions. Arthroscopy. 2002;18:151-5.

11. Spahn G, Kahl E, Mückley T, Hofmann GO, Klinger HM. Arthroscopic knee chondroplasty using a bipolar radiofrequency-based device compared to mechanical shaver: results of a prospective, randomized, controlled study. Knee Surg Sports Traumatol Arthrosc. 2008;16:565-73.

12. Spahn G, Klinger HM, Mückley T, Hofmann GO. Four-year results from a randomized controlled study of knee chondroplasty with concomitant medial meniscectomy: mechanical debridement versus radiofrequency chondroplasty. Arthroscopy. 2010;26:S73-80.

13. Amiel D, Ball ST, Tasto JP. Chondrocyte viability and metabolic activity after treatment of bovine articular cartilage with bipolar radiofrequency: an in vitro study. Arthroscopy. 2004;20:503-10.

14. Caffey S, McPherson E, Moore B, Hedman T, Vangsness CT. Effects of radiofrequency energy on human articular cartilage. Am J Sports Med. 2005;33:1035-9.

15. Cook JL, Kuroki K, Kenter K, Marberry K, Brawner T, Geiger T, et al. Bipolar and monopolar radiofrequency treatment of osteoarthritic knee articular cartilage: acute and temporal effects on cartilage compressive stiffness, permeability, cell synthesis, and extracellular matrix composition. J Knee Surg. 2004;17:99-108.

16. Chu CR, Kaplan LD, Fu FH, Crossett LS, Studer RK. Recovery of articular cartilage metabolism following thermal stress is facilitated by IGF-1 and JNK inhibitor. Am J Sports Med. 2004;32:191-6.

17. Edwards RB, Lu Y, Nho S, Cole BJ, Markel MD. Thermal chondroplasty of chondromalacic human cartilage: an ex vivo comparison of bipolar and monopolar radiofrequency devices. Am J Sports Med. 2002;30:90-7.

18. Kääb MJ, Bail HJ, Rotter A, Mainil-Varlet P, Gwynn I, Weiler A. Monopolar radiofrequency treatment of partial-thickness cartilage defects in the sheep knee joint leads to extended cartilage injury. Am J Sports Med. 2005;33:1472-8.

19. Kaplan LD, Chu CR, Bradley JP, Fu FH, Studer RK. Recovery of chondrocyte metabolic activity after thermal exposure. Am J Sports Med. 2003;31:392-8.

20. Lotto ML, Lu Y, Mitchell ME, Wright EJ, Lubowitz JH, Markel MD. An ex vivo thermal chondroplasty model: the association of a char-like layer and underlying cell death. Arthroscopy. 2006;22:1159-62.

21. Lu Y, Meyer ML, Bogdanske JJ, Markel MD. The effects of radiofrequency energy probe speed and application force on chondrocyte viability. Vet Comp Orthop Traumatol. 2007;20:34-7.

22. Lu Y, Hayashi K, Hecht P, Fanton GS, Thabit G 3rd, Cooley AJ, et al. The effect of monopolar radiofrequency energy on partial-thickness defects of articular cartilage. Arthroscopy. 2000;16:527-36.

23. Uthamanthil RK, Edwards RB, Lu Y, Manley PA, Athanasiou KA, Markel MD. In vivo study on the short-term effect of radiofrequency energy on chondromalacic patellar cartilage and its correlation with calcified cartilage pathology in an equine model. J Orthop Res. 2006;24:716-24.

24. Voss JR, Lu Y, Edwards RB, Bogdanske JJ, Markel MD. Effects of thermal energy on chondrocyte viability. Am J Vet Res. 2006;67:1708-12.

25. Yasura K, Nakagawa Y, Kobayashi M, Kuroki H, Nakamura T. Mechanical and biochemical effect of monopolar radiofrequency energy on human articular cartilage: an in vitro study. Am J Sports Med. 2006;34:1322-7.

26. Broom ND, Ngo T, Tham E. Traversing the intact/fibrillated joint surface: a biomechanical interpretation. J Anat. 2005; 206:55-67.

27. Flachsmann R, Kim W, Broom N. Vulnerability to rupture of the intact articular surface with respect to age and proximity to site of fibrillation: a dynamic and static-investigation. Connect Tissue Res. 2005;46:159-69.

28. Glaser C, Putz R. Functional anatomy of articular cartilage under compressive loading: quantitative aspects of global, local and zonal reactions of the collagenous network with respect to the surface integrity. Osteoarthritis Cartilage. 2002;10:83-99.

29. Kerin AJ, Coleman A, Wisnom MR, Adams MA. Propagation of surface fissures in articular cartilage in response to cyclic loading in vitro. Clin Biomech (Bristol, Avon). 2003;18:960-8.

30. Lewis JL, Johnson SL. Collagen architecture and failure processes in bovine patellar cartilage. J Anat. 2001;199:483-92.

31. Papaioannou G, Demetropoulos CK, King YH. Predicting the effects of knee focal articular surface injury with a patient-specific finite element model. Knee. 2010;17:61-8.

32. Setton LA, Zhu W, Mow VC. The biphasic poroviscoelastic behavior of articular cartilage: role of the surface zone in governing the compressive behavior. J Biomech. 1993;26:581-92.

33. Silver FH, Bradica G, Tria A. Do changes in the mechanical properties of articular cartilage promote catabolic destruction of cartilage and osteoarthritis? Matrix Biol. 2004;23:467-76.

34. Arnoczky SP, moderator. Is there a role for radiofrequency-based ablation in the treatment of chondral lesions? Am J Orthop. 2005;8(Suppl):3-15.

35. Voloshin I, DeHaven KE. A careful technique: using bipolar radiofrequency for treating chondral lesions. Orthop Tech Rev. 2006;Jul/Aug:29-30.

36. Graham WG, Stadler KR. Plasmas in saline solutions. J Phys Conf Ser. 2007;71:012013.

37. Priglinger SG, Palanker D, Alge CS, Kreutzer TC, Haritoglou C, Grueterich M, et al. Pulsed electron avalanche knife: new technology for cataract surgery. Br J Ophthalmol. 2007;91:949-54.

38. Stadler KR, Woloszko J, Brown I, Smith CD. Repetitive plasma discharges in saline solutions. Appl Phys Lett. 2001;79:4503-5.

39. Woloszko J, Stadler KR, Brown IG. Plasma characteristics of repetitively-pulsed electrical discharges in saline solutions used for surgical procedures. IEEE Trans Plasma Sci. 2002;30:1376-83.

40. Tomita M. Involvement of DNA-PK and ATM in radiation- and heat-induced DNA damage recognition and apoptotic cell death. J Radiat Res (Tokyo). 2010;51:493-501.

41. Hong EH, Lee SJ, Kim JS, Lee KH, Um HD, Kim JH, et al. Ionizing radiation induces cellular senescence of articular chondrocytes via negative regulation of SIRT1 by p38 kinase. J Biol Chem. 2010;285:1283-95.

42. Schönmeyr BH, Wong AK, Soares M, Fernandez J, Clavin N, Mehrara BJ. Ionizing radiation of mesenchymal stem cells results in diminution of the precursor pool and limits potential for multilineage differentiation. Plast Reconstr Surg. 2008;122:64-76.

43. Dowthwaite GP, Bishop JC, Redman SN, Khan IM, Rooney P, Evans DJ, et al. The surface of articular cartilage contains a progenitor cell population. J Cell Sci. 2004;117:889-97.

44. Hattori S, Oxford C, Reddi AH. Identification of superficial zone articular chondrocyte stem/progenitor cells. Biochem Biophys Res Commun. 2007;358:99-103.

45. Hayes AJ, Dowthwaite GP, Webster SV, Archer CW. The distribution of notch receptors and their ligands during articular cartilage development. J Anat. 2003;202:495-502.

46. Martin JM, Smith M, Al-Rubeai M. Cryopreservation and in vitro expansion of chondroprogenitor cells isolated from the superficial zone of articular cartilage. Biotechnol Prog. 2005;21:168-77.

47. Grogan SP, Miyaki S, Asahara H, D'Lima DD, Lotz MK. Mesenchymal progenitor cell markers in human articular cartilage: normal distribution and changes in osteoarthritis. Arthritis Res Ther. 2009;11:R85.

48. Cornelissen M, Thierens H, De Ridder L. Effects of ionizing radiation on cartilage: emphasis on effects on the extracellular matrix. Scanning Microsc. 1996;10:833-40.

49. Archer CW, Redman S, Khan I, Bishop J, Richardson K. Enhancing tissue integration in cartilage repair procedures. J Anat. 2006;209:481-93.

50. Gilbert SJ, Singhrao SK, Khan IM, Gonzalez LG, Thomson BM, Burdon D, et al. Enhanced tissue integration during cartilage repair in vitro can be achieved by inhibiting chondrocyte death at the wound edge. Tissue Eng Part A. 2009;15:1739-49.

51. Grogan SP, Olee T, Hiraoka K, Lotz MK. Repression of chondrogenesis through binding of notch signaling proteins HES-1 and HEY-1 to N-box domains in the COL2A1 enhancer site. Arthritis Rheum. 2008;58:2754-63.

52. Hayes AJ, Hall A, Cheung I, Brown L, Tubo R, Caterson B. Surface zone but not deep zone chondrocytes reorganize zonal architecture of articular cartilage grafts grown in vitro. Transactions of the Orthopaedic Research Society; Vol. 30, Poster 1774; 2005 February 20-23; Washington, DC.

53. Hayes AJ, MacPherson S, Morrison H, Dowthwaite G, Archer CW. The development of articular cartilage: evidence for an appositional growth mechanism. Anat Embryol (Berl). 2001;203:469-79.

54. Hunziker EB, Kapfinger E. Removal of proteoglycans from the surface of defects in articular cartilage transiently enhances coverage by repair cells. J Bone Joint Surg Br. 1998;80:144-50.

55. Karlsson C, Lindahl A. Articular cartilage stem cell signaling. Arthritis Res Ther. 2009;11:121.

56. Kim AC, Spector M. Distribution of chondrocytes containing alpha-smooth muscle actin in human articular cartilage. J Orthop Res. 2000;18:749-55.

57. Rolauffs B, Williams JM, Aurich M, Grodzinsky AJ, Kuettner KE, Cole AA. Proliferative remodeling of the spatial organization of human superficial chondrocytes distant from focal early osteoarthritis. Arthritis Rheum. 2010;62:489-98.

58. McRury ID, Morgan RE, Augé WK. The manipulation of water with non-ablation radiofrequency energy: a repetitive molecular energy conversion loop under non-ionizing electromagnetic forces. Water. 2010;2:108-32.

59. Augé WK. The intimate relationships between tissue surface barriers and their saline environments create a therapeutic substrate for the surgical rescue of diseased tissue: a molecular energy conversion loop designed for surgical work. Proceedings of the World Congress of Marine Biotechnology: Biomedical Applications

of Marine Biotechnology; 2011 April 25-29; Dalian, China.

60. Augé WK. Addressing the large world-wide disease burden of osteoarthritis through targeted induction of biosynthetic gene expression: early intervention engineered to reverse articular cartilage lesions. Proceedings of the World DNA and Genome Day: Human Genetics and Diseases; 2011 April 25-29; Dalian, China.

61. Katrantzis M, Baker MS, Handley CJ, Lowther DA. The oxidant hypochlorite (OCL-), a product of the myeloperoxidae system, degrades articular cartilage proteoglycan aggregate. Free Radic Biol Med. 1991;10:101-9.

62. Sandy JD, Plaas AH. Studies on the hyaluronate binding properties of newly synthesized proteoglycans purified from articular chondrocyte cultures. Arch Biochem Biophys. 1989;271:300-14.

63. Schiller J, Arnhold J, Gründer W, Arnold K. The action of hypochlorous acid on polymeric components of cartilage. Biol Chem Hoppe Seyler. 1994;375:167-72.

64. Livesay DR, Huynh DH, Dallakyan S, Jacobs DJ. Hydrogen bond networks determine emergent mechanical and thermodynamic properties across a protein family. Chem Cent J. 2008;2:17.

65. Loret B, Simões FM. Effects of pH on transport properties of articular cartilages. Biomech Model Mechanobiol. 2010;9:45-63.

66. Loret B, Simões FM. Mechanical effects of ionic replacements in articular cartilage, part II: simulations of successive substitutions of NaCl and CaCl(2). Biomech Model Mechanobiol. 2005;4:81-99.

67. Loret B, Simões FM. Mechanical effects of ionic replacements in articular cartilage, part I: the constitutive model. Biomech Model Mechanobiol. 2005;4:63-80.

68. Olszowski S, Mak P, Olszowska E, Marcinkiewicz J. Collagen type II modification by hypochlorite. Acta Biochim Pol. 2003;50:471-9.

69. Teixeira J. Dynamics of hydration water in proteins. Gen Physiol Biophys. 2009;28:168-73.

70. June RK, Mejia KL, Barone JR, Fyhrie DP. Cartilage stress-relaxation is affected by both the charge concentration and valence of solution cations. Osteoarthritis Cartilage. 2009;17:669-76.

71. Korhonen RK, Herzog W. Depth-dependent analysis of the role of collagen fibrils, fixed charges and fluid in the pericellular matrix of articular cartilage on chondrocyte mechanics. J Biomech. 2008;41:480-5.

72. Korhonen RK, Julkunen P, Wilson W, Herzog W. Importance of collagen orientation and depth-dependent fixed charge densities of cartilage on mechanical behavior of chondrocytes. J Biomech Eng. 2008;130:021003.

73. Korhonen RK, Jurvelin JS. Compressive and tensile properties of articular cartilage in axial loading are modulated differently by osmotic environment. Med Eng Phys. 2010;32:155-60.

74. Likhitpanichkul M, Guo XE, Mow VC. The effect of matrix tension-compression nonlinearity and fixed negative charges on chondrocyte responses in cartilage. Mol Cell Biomech. 2005;2:191-204.

75. Lu XL, Mow VC. Biomechanics of articular cartilage and determination of material properties. Med Sci Sports Exerc. 2008;40:193-9.

76. Lu XL, Wan LQ, Guo XE, Mow VC. A linearized formulation of triphasic mixture theory for articular cartilage, and its application to indentation analysis. J Biomech. 2010;43:673-9.

77. Sun DD, Guo XE, Likhitpanichkul M, Lai WM, Mow VC. The influence of the fixed negative charges on mechanical and electrical behaviors of articular cartilage under unconfined compression. J Biomech Eng. 2004;126:6-16.

78. Wachtel E, Maroudas A. The effects of pH and ionic strength on intrafibrillar hydration in articular cartilage. Biochim Biophys Acta. 1998;1381:37-48.

79. Wan LQ, Guo XE, Mow VC. A triphasic orthotropic laminate model for cartilage curling behavior: fixed charge density versus mechanical properties inhomogeneity. J Biomech Eng. 2010;132:024504.

80. Gratz KR, Wong BL, Bae WC, Sah RL. The effects of focal articular defects on intra-tissue strains in the surrounding and opposing cartilage. Biorheology. 2008;45:193-207.

81. Nguyen QT, Wong BL, Chun J, Yoon YC, Talke FE, Sah RL. Macroscopic assessment of cartilage shear: effects of countersurface roughness, synovial fluid lubricant, and compression offset. J Biomech. 2010;43:1787-93.

82. Spirt AA, Mak AF, Wassell RP. Nonlinear viscoelastic properties of articular cartilage in shear. J Orthop Res. 1989;7:43-9.

83. Wang Q, Zheng YP, Niu HJ. Changes in triphasic mechanical properties of proteoglycan-depleted articular cartilage extracted from osmotic swelling behavior monitored using high-frequency ultrasound. Mol Cell Biomech. 2010;7:45-58.

84. Wong BL, Bae WC, Gratz KR, Sah RL. Shear deformation kinematics during cartilage articulation: effect of lubrication, degeneration, and stress relaxation. Mol Cell Biomech. 2008;5:197-206.

85. Wu MH, Urban JP, Cui ZF, Cui Z, Xu X. Effect of extracellular ph on matrix synthesis by chondrocytes in 3D agarose gel. Biotechnol Prog. 2007;23:430-4.

86. Hills BA. Boundary lubrication in vivo. Proc Inst Mech Eng H. 2000;214:83-94.

87. United States Department of Energy. The ethical, legal, and social issues research (ELSI) program. The Human Genome Project: Biological and Environmental Research Information System (BERIS). Available from: http://www.genomics. energy.gov, http://www.ornl.gov/sci/techresources/Human _Genome/elsi/elsi.shtml, and http://www.lanl.gov/orgs/pa/ science21/HumanGenome.html.

88. Polacek M, Bruun JA, Johansen O, Martinez I. Differences in the secretome of cartilage explants and cultured chondrocytes unveiled by SILAC technology. J Orthop Res. 2010;28:1040-9.

89. Matsumoto K, Kamiya N, Suwan K, Atsumi F, Shimizu K, Shinomura T, *et al*. Identification and characterization of versican/PG-M aggregates in cartilage. J Biol Chem. 2006;281:18257-63.

90. Sztrolovics R, Grover J, Cs-Szabo G, Shi SL, Zhang Y, Mort JS, *et al*. The characterization of versican and its message in human articular cartilage and intervertebral disc. J Orthop Res. 2002;20:257-66.

91. Hayes AJ, Tudor D, Nowell MA, Caterson B, Hughes CE. Chondroitin sulfate sulfation motifs as putative biomarkers for isolation of articular cartilage progenitor cells. J Histochem Cytochem. 2008;56:125-38.

92. Sandell LJ, Aigner T. Articular cartilage and changes in arthritis: cell biology of osteoarthritis. Arthritis Res. 2001;3:107-13.

93. Nishida K, Inoue H, Murakami T. Immunohistochemical demonstration of fibronectin in the most superficial layer of normal rabbit articular cartilage. Ann Rheum Dis. 1995;54:995-8.

94. Montella A, Manunta A, Espa E, Gasparini G, De Santis E, Gulisano M. Human articular cartilage in osteoarthrosis, I: the matrix. Transmission electron microscopic study. Ital J Anat Embryol. 1992;97:1-12.

95. Crockett R. Boundary lubrication in natural articular joints. Tribol Lett. 2009;35:77-84.

96. Kumar P, Oka M, Toguchida J, Kobayashi M, Uchida E, Nakamura T, *et al*. Role of uppermost superficial surface layer of articular cartilage in the lubrication mechanism of joints. J Anat. 2001;199:241-50.

97. Crockett R, Grubelnik A, Roos S, Dora C, Born W, Troxler H. Biochemical composition of the superficial layer of articular cartilage. J Biomed Mater Res A. 2007;82:958-64.

98. Pawlak Z, Oloyede A. Conceptualisation of articular cartilage as a giant reverse micelle: a hypothetical mechanism for joint biocushioning and lubrication. Biosystems. 2008;94:193-201.

99. Pawlak Z, Kotynska J, Figaszewski ZA, Gadomski A, Gudaniec A, Oloyede A. A biochemical model for characterising the surface-active phospholipid bilayer of articular cartilage relative to acid-base equilibrium. Arch Mat Sci Eng. 2008;20:24-9.

100. Pawlak Z, Figaszewskic ZA, Gadomskid A, Urbaniakb W, Oloyedee A. The ultra-low friction of the articular surface is pH-dependent and is built on a hydrophobic underlay including a hypothesis on joint lubrication mechanism. Tribol Int. 2010;43:1719-25.

101. Choocheep K, Hatano S, Takagi H, Watanabe H, Kimata K, Kongtawelert P, *et al*. Versican facilitates chondrocyte differentiation and regulates joint morphogenesis. J Biol Chem. 2010;285:21114-25.

102. Hudson KS, Andrews K, Early J, Mjaatvedt CH, Capehart AA. Versican G1 domain and V3 isoform overexpression results in increased chondrogenesis in the developing chick limb in ovo. Anat Rec (Hoboken). 2010;293:1669-78.

103. Kamiya N, Watanabe H, Habuchi H, Takagi H, Shinomura T, Shimizu K, *et al*. Versican/PG-M regulates chondrogenesis as an extracellular matrix molecule crucial for mesenchymal condensation. J Biol Chem. 2006;281:2390-400.

104. Shepard JB, Gliga DA, Morrow AP, Hoffman S, Capehart AA. Versican knock-down compromises chondrogenesis in the embryonic chick limb. Anat Rec (Hoboken). 2008;291:19-27.

105. Wu Y, Wu J, Lee DY, Yee A, Cao L, Zhang Y, *et al*. Versican protects cells from oxidative stress-induced apoptosis. Matrix Biol. 2005;24:3-13.

106. Zhang Y, Cao L, Kiani C, Yang BL, Hu W, Yang BB. Promotion of chondrocyte proliferation by versican mediated by G1 domain and EGF-like motifs. J Cell Biochem. 1999;73:445-57.

107. Schnabel M, Marlovits S, Eckhoff G, Fichtel I, Gotzen L, Vécsei V, *et al*. Dedifferentiation-associated changes in morphology and gene expression in primary human articular chondrocytes in cell culture. Osteoarthritis Cartilage. 2002;10:62-70.

108. Dehne T, Schenk R, Perka C, Morawietz L, Pruss A, Sittinger M, *et al*. Gene expression profiling of primary human articular chondrocytes in high-density micromasses reveals patterns of recovery, maintenance, re- and dedifferentiation. Gene. 2010;462:8-17.

109. Aigner T, Zhu Y, Chansky HH, Matsen FA 3rd, Maloney WJ, Sandell LJ. Reexpression of type IIA procollagen by adult articular chondrocytes in osteoarthritic cartilage. Arthritis Rheum. 1999;42:1443-50.

110. Nollen EA, Morimoto RI. Chaperoning signaling pathways: molecular chaperones as stress-sensing 'heat shock' proteins. J Cell Sci. 2002;115:2809-16.

111. Tonomura H, Takahashi KA, Mazda O, Arai Y, Shin-Ya M, Inoue A, *et al*. Effects of heat stimulation via microwave applicator on cartilage matrix gene and HSP70 expression in the rabbit knee joint. J Orthop Res. 2008;26:34-41.

112. Wang S, Diller KR, Aggarwal SJ. Kinetics study of endogenous heat shock protein 70 expression. J Biomech Eng. 2003;125:794-7.

113. Terauchi R, Takahashi KA, Arai Y, Ikeda T, Ohashi S, Imanishi J, *et al*. Hsp70 prevents nitric oxide-induced apoptosis in articular chondrocytes. Arthritis Rheum. 2003;48:1562-8.

114. Sawatzky DA, Foster R, Seed MP, Willoughby DA. Heat-shock proteins and their role in chondrocyte protection, an application for autologous transplantation. Inflammopharmacology. 2005;12:569-89.

115. Etienne S, Gaborit N, Henrionnet C, Pinzano A, Galois L, Netter P, *et al*. Local induction of heat shock protein 70 (Hsp70) by proteasome inhibition confers chondroprotection during surgically induced osteoarthritis in the rat knee. Biomed Mater Eng. 2008;18:253-60.

116. Grossin L, Cournil-Henrionnet C, Pinzano A, Gaborit N, Dumas D, Etienne S, *et al*. Gene transfer with HSP 70 in rat chondrocytes confers cytoprotection in vitro and during experimental osteoarthritis. FASEB J. 2006;20:65-75.

117. Lambrecht S, Dhaenens M, Almqvist F, Verdonk P, Verbruggen G, Deforce D, *et al*. Proteome characterization of human articular chondrocytes leads to novel insights in the function of small heat-shock proteins in chondrocyte homeostasis. Osteoarthritis Cartilage. 2010;18:440-6.

118. Otsuka G, Kubo T, Imanishi J, Hirasawa Y. Expression of heat-shock-proteins in the differentiation process of chondrocytes. Nippon Geka Hokan. 1996;65:39-48.

119. Takahashi K, Kubo T, Arai Y, Imanishi J, Kawata M, Hirasawa Y. Localization of heat shock protein in osteoarthritic cartilage. Scand J Rheumatol. 1997;26:368-75.

120. Takahashi K, Kubo T, Goomer RS, Amiel D, Kobayashi K, Imanishi J, *et al*. Analysis of heat shock proteins and cytokines expressed during early stages of osteoarthritis in a mouse model. Osteoarthritis Cartilage. 1997;5:321-9.

121. Zhang Z, Fan J, Becker KG, Graff RD, Lee GM, Francomano CA. Comparison of gene expression profile between human chondrons and chondrocytes: a cDNA microarray study. Osteoarthritis Cartilage. 2006;14:449-59.

122. Bachrach NM, Valhmu WB, Stazzone E, Ratcliffe A, Lai WM, Mow VC. Changes in proteoglycan synthesis of chondrocytes in articular cartilage are associated with the time-dependent changes in their mechanical environment. J Biomech. 1995;28:1561-9.

123. Brew CJ, Clegg PD, Boot-Handford RP, Andrew JG, Hardingham T. Gene expression in human chondrocytes in late osteoarthritis is changed in both fibrillated and intact cartilage without evidence of generalised chondrocyte hypertrophy. Ann Rheum Dis. 2010;69:234-40.

124. Fitzgerald JB, Jin M, Grodzinsky AJ. Shear and compression differentially regulate clusters of functionally related temporal transcription patterns in cartilage tissue. J Biol Chem. 2006;281:24095-103.

125. Mauck RL, Byers BA, Yuan X, Tuan RS. Regulation of cartilaginous ECM gene transcription by chondrocytes and MSCs in 3D culture in response to dynamic loading. Biomech Model Mechanobiol. 2007;6:113-25.

126. Lee JH, Fitzgerald JB, DiMicco MA, Grodsinsky AJ. Mechanical injury of cartilage explants causes specific time-dependent changes in chondrocyte gene expression. Arthritis Rheum. 2005;52:2386-95.

127. Sironen R, Elo M, Kaarniranta K, Helminen HJ, Lammi MJ. Transcriptional activation in chondrocytes submitted to hydrostatic pressure. Biorheology. 2000;37:85-93.

128. Valhmu WB, Stazzone EJ, Bachrach NM, Saed-Nejad F, Fischer SG, Mow VC, *et al*. Load-controlled compression of articular cartilage induces a transient stimulation of aggrecan gene expression. Arch Biochem Biophys. 1998;353:29-36.

129. Kaarniranta K, Holmberg CI, Lammi MJ, Eriksson JE, Sistonen L, Helminen HJ. Primary chondrocytes resist hydrostatic pressure-induced stress while primary synovial cells and fibroblasts show modified Hsp70 response. Osteoarthritis Cartilage. 2001;9:7-13.

130. Madreperla SA, Louwerenburg B, Mann RW, Towle CA, Mankin HJ, Treadwell BV. Induction of heat-shock protein synthesis in chondrocytes at physiological temperatures. J Orthop Res. 1985;3:30-5.

131. Miles CA, Bailey AJ. Thermally labile domains in the collagen molecule. Micron. 2001;32:325-32.

132. Miles CA, Avery NC, Rodin VV, Bailey AJ. The increase in denaturation temperature following cross-linking of collagen is caused by dehydration of the fibres. J Mol Biol. 2005;346:551-6.

133. Das RH, van Osch GJ, Kreukniet M, Oostra J, Weinans H, Jahr H. Effects of individual control of pH and hypoxia in chondrocyte culture. J Orthop Res. 2010;28:537-45.

134. Ganguly K, Rasmussen KØ, Alexandrov BS, Bishop AR, Goodwin PM, Augé WK. Nanomedical DNA conduction: accessing genomic control mechanisms associated with biosynthetic tissue assembly. Proceedings of The Ninth International Nanomedicine and Drug Delivery Symposium. Salt Lake City, Utah. October 15-16, 2011.

135. Challis LJ. Mechanisms for interaction between RF fields and biological tissue. Bioelectromagnetics. 2005;7:S98-106.

136. Funk RH, Monsees T, Ozkucur N. Electromagnetic effects: from cell biology to medicine. Prog Histochem Cytochem. 2009;43:177-264.

137. Gordon GA. Extrinsic electromagnetic fields, low frequency phonon vibrations, and control of cell function: a non-linear resonance system. J Biomed Sci Eng. 2008;1:152-6.

138. Sheppard AR, Swicord ML, Balzano Q. Quantitative evaluations of mechanisms of radiofrequency interactions with biological molecules and processes. Health Phys. 2008;95:365-96.

139. Szasz A, Vincze G, Andocs G, Szasz O. Do field-free electromagnetic potentials play a role in biology? Electromagn Biol Med. 2009;28:135-47.

140. Weaver JC. Understanding conditions for which biological effects of nonionizing electromagnetic fields can be expected. Bioelectrochemistry. 2002;56:207-9.

141. Sánchez JC, Powell T, Staines HM, Wilkins RJ. Electrophysiological demonstration of voltage-activated H+ channels in bovine articular chondrocytes. Cell Physiol Biochem. 2006;18:85-90.

142. Haila S, Hästbacka J, Böhling T, Karjalainen-Lindsberg ML, Kere J, Saarialho-Kere U. SLC26A2 (diastrophic dysplasia sulfate transporter) is expressed in developing and mature cartilage but also in other tissues and cell types. J Histochem Cytochem. 2001;49:973-82.

143. Levin M. Large-scale biophysics: ion flows and regeneration. Trends Cell Biol. 2007;17:261-70.

144. Aaron RK, Ciombor DM, Wang S, Simon B. Clinical biophysics: the promotion of skeletal repair by physical forces. Ann N Y Acad Sci. 2006;1068:513-31.

145. Brighton CT, Wang W, Clark CC. The effect of electrical fields on gene and protein expression in human osteoarthritic cartilage explants. J Bone Joint Surg Am. 2008;90:833-48.

146. Chang CH, Loo ST, Liu HL, Fang HW, Lin HY. Can low frequency electromagnetic field help cartilage tissue engineering? J Biomed Mater Res A. 2010;92:843-51.

147. Ciombor DM, Lester G, Aaron RK, Neame P, Caterson B. Low frequency EMF regulates chondrocyte differentiation and expression of matrix proteins. J Orthop Res. 2002;20:40-50.

148. Fini M, Torricelli P, Giavaresi G, Aldini NN, Cavani F, Setti S, *et al*. Effect of pulsed electromagnetic field stimulation on knee cartilage, subchondral and epyphiseal trabecular bone of aged Dunkin Hartley guinea pigs. Biomed Pharmacother. 2008;62:709-15.

149. MacGinitie LA, Gluzband YA, Grodzinsky AJ. Electric field stimulation can increase protein synthesis in articular cartilage explants. J Orthop Res. 1994;12:151-60.

150. Massari L, Benazzo F, De Mattei M, Setti S, Fini M; CRES Study Group. Effects of electrical physical stimuli on articular cartilage. J Bone Joint Surg Am. 2007;89:S152-61.

151. Wang W, Wang Z, Zhang G, Clark CC, Brighton CT. Up-regulation of chondrocyte matrix genes and products by electric fields. Clin Orthop Relat Res. 2004;427:S163-73.

152. Xu J, Wang W, Clark CC, Brighton CT. Signal transduction in electrically stimulated articular chondrocytes involves translocation of extracellular calcium through voltage-gated channels. Osteoarthritis Cartilage. 2009;1:397-405.

153. Blank M, Goodman R. Electromagnetic fields stress living cells. Pathophysiology. 2009;16:71-8.

154. Blank M, Goodman R. Initial interactions in electromagnetic field-induced biosynthesis. J Cell Physiol. 2004;199:359-63.

155. Vonk LA, Doulabi BZ, Huang C, Helder MN, Everts V, Bank RA. Preservation of the chondrocyte's pericellular matrix improves cell-induced cartilage formation. J Cell Biochem. 2010;110:260-71.

156. McGlashan SR, Cluett EC, Jensen CG, Poole CA. Primary cilia in osteoarthritic chondrocytes: from chondrons to clusters. Dev Dynamics. 2008;237:2013-20.

157. van der Kraan PM, Buma P, van Kuppevelt T, van den Berg WB. Interaction of chondrocytes, extracellular matrix and growth factors: relevance for articular cartilage tissue engineering. Osteoarthritis Cartilage. 2002;10:631-7.

158. Bay-Jensen AC, Hoegh-Madsen S, Dam E, Henriksen K, Sondergaard BC, Pastoureau P, *et al*. Which elements are involved in reversible and irreversible cartilage degradation in osteoarthritis? Rheumatol Int. 2010;30:435-42.

159. Burstein D. Tracking longitudinal changes in knee degeneration and repair. J Bone Joint Surg Am. 2009;91:S51-3.

160. Ding C, Jones G, Wluka AE, Cicuttini F. What can we learn about osteoarthritis by studying a healthy person against a person with early onset of disease? Curr Opin Rheumatol. 2010;22:520-7.

161. Ballantine GC, Stachowiak GW. The effects of lipid depletion on osteoarthritic wear. Wear. 2002;253:385-93.

162. Saarakkala S, Julkunen P, Kiviranta P, Mäkitalo J, Jurvelin JS, Korhonen RK. Depth-wise progression of osteoarthritis in human articular cartilage: investigation of composition, structure and biomechanics. Osteoarthritis Cartilage. 2010;18:73-81.

163. Graindorge S, Ferrandez W, Ingham E, Jin Z, Twigg P, Fisher J. The role of the surface amorphous layer of articular cartilage in joint lubrication. Proc Inst Mech Eng H. 2006;220:597-607.

164. Lee CH, Cook JL, Mendelson A, Moioli EK, Yao H, Mao JJ. Regeneration of the articular surface of the rabbit synovial joint by cell homing: a proof of concept study. Lancet. 2010;376:440-8.